

Modeling of Ceiling Fan Based on Velocity Measurement for CFD Simulation of Airflow in Large Room

Y. Momoi¹, K. Sagara¹, T. Yamanaka¹ and H. Kotani¹

¹Osaka University, Graduate School of Eng., Dept. of Architectural Eng., 2-1 Yamadaoka, Suita, Osaka, Japan
Email: momoi@arch.eng.osaka-u.ac.jp http://www.arch.eng.osaka-u.ac.jp/~labo4/

Summary: This study examines the way of utilizing a ceiling fan for airflow control in a large air-conditioned room. Although it seems that CFD simulation is useful in predicting the airflow around a ceiling fan, modeling of a ceiling fan as a body of rotation is very complicated. Therefore, in this study, airflow of a ceiling fan is modeled as boundary conditions of air velocity data measured near the ceiling fan. In this paper, the measured airflow pattern around a ceiling fan is compared with the CFD simulation result using the airflow model of the ceiling fan, in order to examine the validity of the airflow model. The CFD result was in good agreement with the measurement result concerning the average of air velocity.

Keywords: Ceiling fan, CFD, Boundary condition, Measurement data, Large room

Category: Modeling techniques

1. Introduction

This study examines the way of utilizing a ceiling fan [1, 2, 3] in a large air-conditioned room for the dissolution of an indoor vertical temperature gradient in winter and the prevention of draft in summer. Although it seems that Computational Fluid Dynamics (CFD) simulation is useful in predicting the airflow around a ceiling fan, modeling of a ceiling fan as a body of rotation is very complicated. Since the number of divisions of the space increases, calculation load becomes heavy. As for complex-shaped supply openings, some techniques of modeling and decreasing calculation load are proposed by Nielsen [4]. In this study, these techniques will be applied to a ceiling fan, and airflow of a ceiling fan is modeled as the boundary conditions based on velocity data measured near the ceiling fan.

In this paper, the measured airflow pattern around the ceiling fan is compared with the CFD simulation result using the airflow model of the ceiling fan, in order to examine the validity of the airflow model.

2. Airflow model of ceiling fan

A ceiling fan (Matsushita Electric Industrial, F-M131H-W) used in this research is shown in Fig.1. In the CFD simulation of an indoor airflow induced by this ceiling fan, two virtual planes whose each side length is 140 cm are assumed at the position of 20cm above and below the ceiling fan. Measured values of air velocity and turbulent parameters near the ceiling fan are given as boundary conditions for airflow of the ceiling fan (Fig.2). The influence of a ceiling fan on an indoor airflow can be taken into consideration in the CFD simulation. It becomes unnecessary to simulate correctly the space between two planes where airflow is complicated in reality, and calculation load can be reduced.

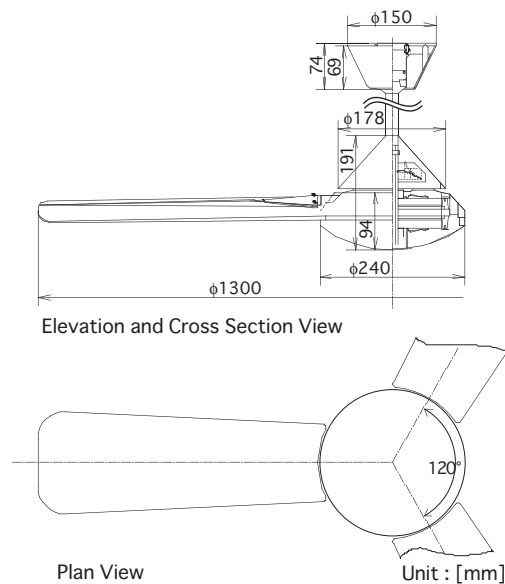


Fig.1 Ceiling fan

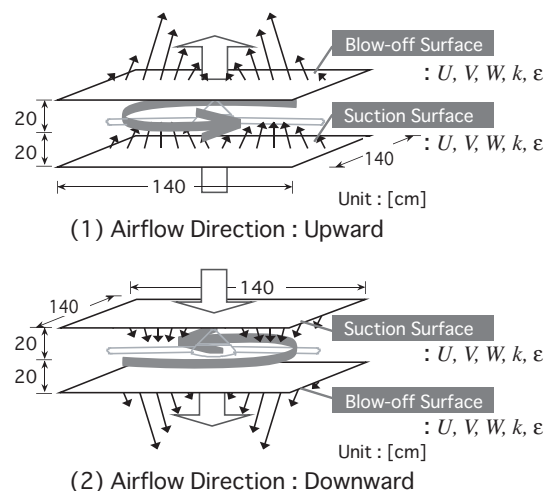


Fig.2 Schematic diagram of airflow model of ceiling fan

3. Experimental set-up

The experiments were carried out in the large experimental room. The iron framework with dimensions of 3.0m x 1.5m x 3.0m was constructed and the ceiling fan with a rotational radius of 65 cm was installed in the height of 2 m above the floor level (Fig.3). Measurement for 30 seconds was performed by 10Hz of sampling frequencies using the 3-dimensional ultrasonic anemometer (KAIJO, WA-590), and the average value of each air velocity component was calculated. Measurement for 20 seconds was carried out by 250Hz of sampling frequencies using hot-wire anemometer of constant temperature type ($\phi 5\mu\text{m}$ tungsten, KANOMAX JAPAN, 0251 R-T5), and turbulent kinetic energy k [m^2/s^2] and energy dissipation of it ε [m^2/s^3] were computed from the auto-correlation of measured air velocities. Measurement was performed at intervals of 5cm or 10cm. The measuring field was set between 80 cm above the ceiling fan and 120 cm below it, and horizontally up to 120 cm from the rotational center of the ceiling fan at each point of the cross section passing through the center of the ceiling fan (see Fig.4). The speed of rotation was fixed at 160 rpm. As the ceiling fan can generate either upward or downward flow depending on the rotational direction, the measurements were conducted under the two experimental conditions that airflow directions from the ceiling fan were upward and downward (Table 1).

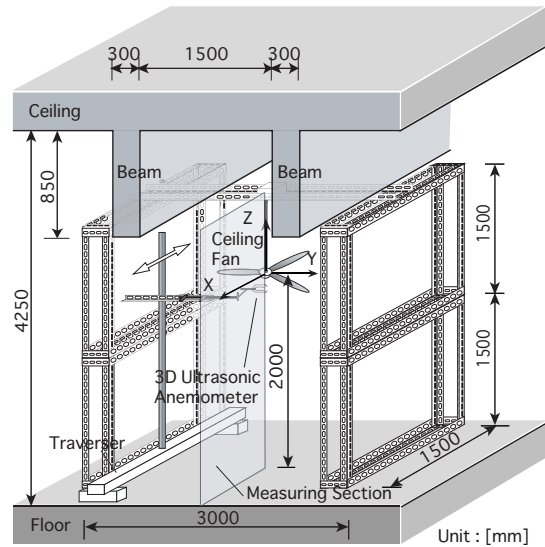


Fig.3 Experimental equipment

4. Boundary Condition

First, regression curves were obtained from the measured velocity data on the line (see Fig.5). Second, the boundary surface set at the position of 20cm above and below the ceiling fan was divided into the mesh of 1cm interval, and the values of air velocity components and turbulent parameters in the central point of each mesh were computed using the regression curves. Finally, the values given to a boundary surface were acquired by averaging them in 10cm mesh. The application section of a regression formula was divided considering the rotational radius ($X=65\text{cm}$) and the position where measured air velocity was the maximum value (upward: $X=35\text{cm}$, downward: $X=45\text{cm}$). All regression formulae were taken as a cubic function. In this way, the boundary conditions on the meshed plane of CFD simulation are determined. The boundary conditions under downward condition and upward condition are shown in Fig.6.

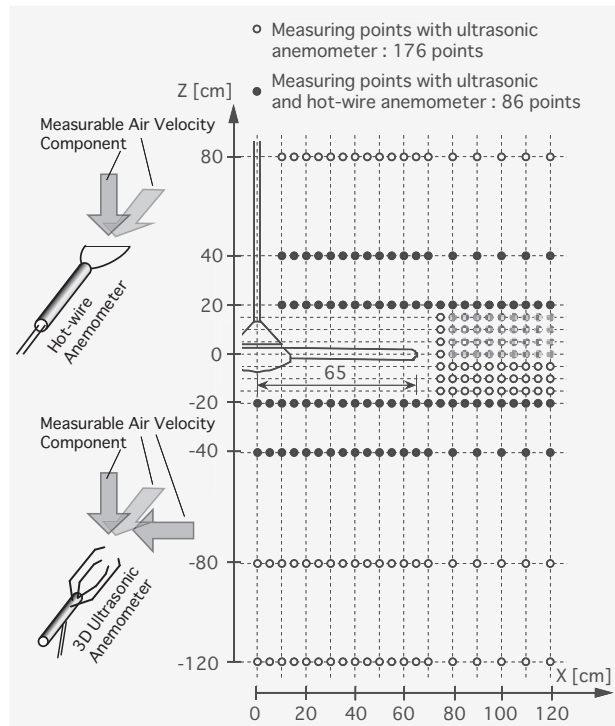


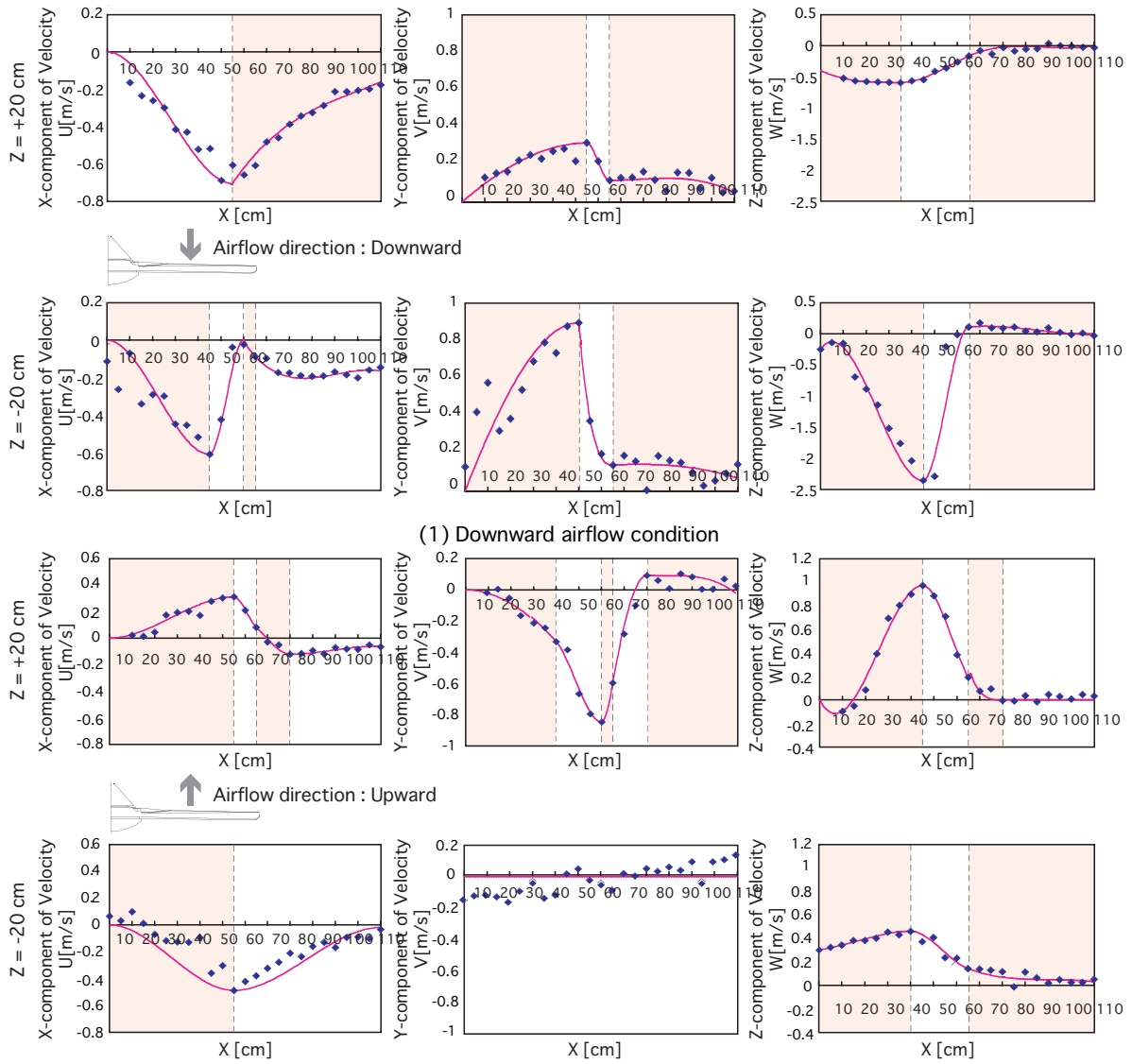


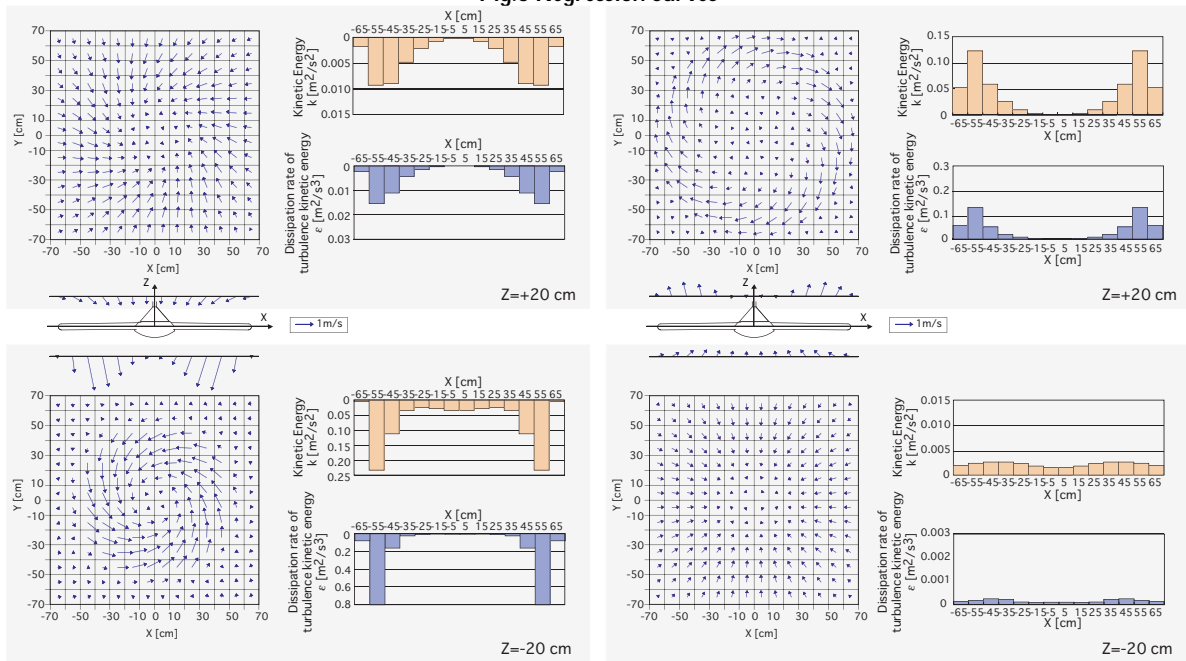
Fig.4 Measuring points

Table 1 Experimental condition

Airflow direction	 
Speed of rotation	160 rpm



(1) Downward airflow condition
 (2) Upward airflow condition
Fig.5 Regression curves



(1) Downward airflow condition
 (2) Upward airflow condition
Fig.6 Boundary conditions

5. CFD simulation set-up

As shown in Fig.7, CFD simulation of the airflow in experimental room was performed using the above-mentioned boundary condition for the ceiling fan based on measured value. The size of simulation space was determined by preliminary simulation. It is large enough to avoid the influence of a wall on the airflow near the ceiling fan.

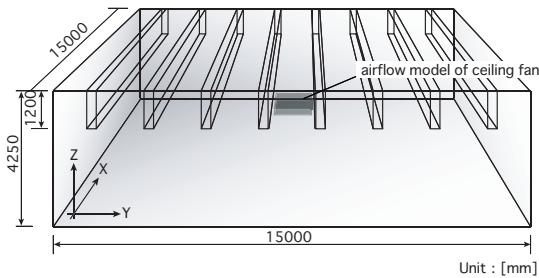
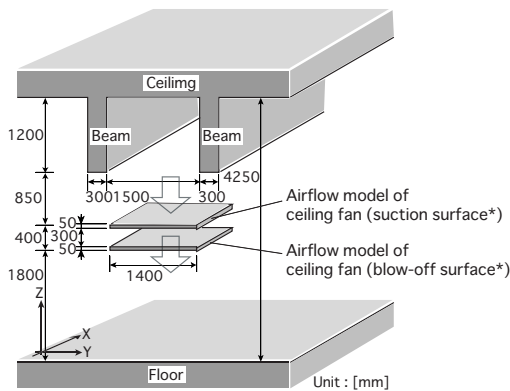


Fig.7 Simulation space



* Under downward airflow condition. When the airflow direction is upward conversely, the upper surface is "Blow-off Surface" and the downer surface is "Suction Surface".

Fig.8 Cross section around ceiling fan

The cross section around the ceiling fan is shown in Fig.8. Beams were arranged with at intervals of 150cm. The airflow model of the ceiling fan was installed in the middle between two beams. On account of the restriction of simulation software, the boundary conditions of the blow-off and suction airflow of the ceiling fan could not be given on one surface respectively, but the same boundary conditions are given to the upper and lower sides of a box with a height of 5cm (the inside of the box was excluded from the simulation space). That is, for example under downward airflow condition, the blow-off surfaces were set at the position of 180cm ($Z=-20\text{cm}$) and 185cm ($Z=-15\text{cm}$) from the floor, and the suction surfaces were set at 215cm ($Z=+15\text{cm}$) and 220cm ($Z=+20\text{cm}$) from the floor. Although the iron framework was constructed around the ceiling fan in the experiment, it was not taken into consideration in the simulation since it appears that the framework does not affect the airflow near the ceiling fan. Simulation field was assumed to be isothermal so that temperature field was not analyzed.

CFD simulations were carried out with the commercial CFD code (STREAM ver.5, Software Cradle co. Ltd. [5]). The standard $k-\varepsilon$ two-equation turbulence model and SIMPLEC algorithm were applied with standard log-law wall function and finite-volume resolution. A computational grid was set up with 10cm interval.

6. Comparison between the measurement and CFD result

6.1 Air velocity distribution

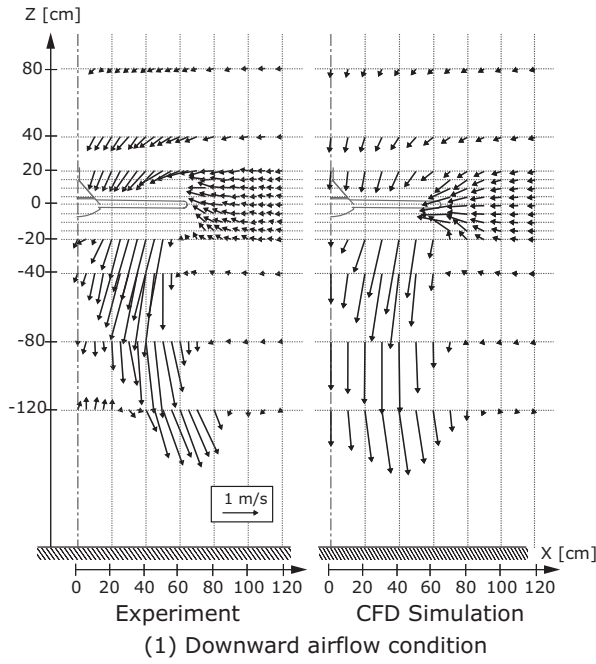
The measurement and CFD result of air velocity under downward condition and upward condition are shown in Fig.9.

(1) Downward airflow condition

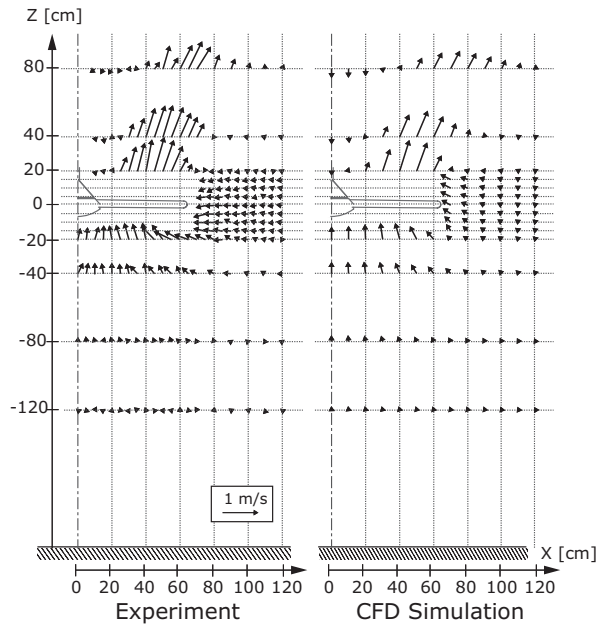
In both measurement and CFD result, it is seen that the airflow goes toward the rotational center of the ceiling fan ($X=0\text{cm}$) at $Z=-20\text{cm}$ (blow-off side). Although the maximum downward air velocity is about 2m/s near $X=45\text{cm}$, air velocity falls suddenly outside it and becomes almost 0m/s outside the rotational radius of the ceiling fan ($X=65\text{cm}$). At $Z=-40\text{cm}$, -80cm , and -120cm in the measurement result, it turns out that the direction of blow-off airflow is changing outward gradually as it becomes far from a ceiling fan. There seems to be the influence of the floor at 200cm under the ceiling fan. However, in the CFD result, such a change of airflow direction observed in the measurement result can't be seen. The downward flow was struck on the floor and changed the upward flow near the rotational center in the measurement result. The upward airflow caused by rebounding of the downward flow was not observed at $Z=-120\text{cm}$ near the rotational center in the CFD result. The insufficient grid division in the CFD field might cause this inconsistency.

(2) Upward airflow condition

In both measurement result and CFD result, in $Z=20\text{cm}$ (blow-off side), the maximum upward air velocity is about 1 m/s near $X=45\text{cm}$. Outward flow is observed as a whole. Outside $X=65\text{cm}$, air velocity was almost 0cm/s. At the height of $Z=40\text{cm}$ and 80cm , it turns out that the airflow blown by the ceiling fan has spread outside since the peak of air velocity distribution is moving outside while upward flow becomes weaker. In a suction side, the horizontal airflow changed into the perpendicular airflow as the airflow approaches the rotational center of the ceiling fan, and the airflow was sucked toward the blades of the ceiling fan. In the outer side of the ceiling fan, the horizontal suction flow that goes to the center of the ceiling fan can be seen. The influence of suction toward the ceiling fan becomes small as it becomes far from the ceiling fan. Concerning the suction flow of the ceiling fan, the CFD and measurement results are enough in agreement and it would be said that it is analyzable with sufficient accuracy.



(1) Downward airflow condition



(2) Upward airflow condition

Fig.9 Air velocity distribution

6.2 Distribution of turbulent kinetic energy and its dissipation rate

Turbulent kinetic energy can be calculated as follows:

$$k = \frac{1}{2} \times \left(\frac{3}{2} \overline{u'^2} \right)$$

and its dissipation rate is given by:

$$\varepsilon = C_D \frac{k^{\frac{3}{2}}}{\ell}$$

Turbulent length is expressed as follows:

$$\ell = C_D^{\frac{1}{4}} \Lambda$$

Λ is integral length and obtained from the auto-correlation of measured air velocities:

$$\Lambda = \bar{u} \int_0^{\infty} \frac{u'(t)u'(t+\tau)}{u'^2(t)} d\tau$$

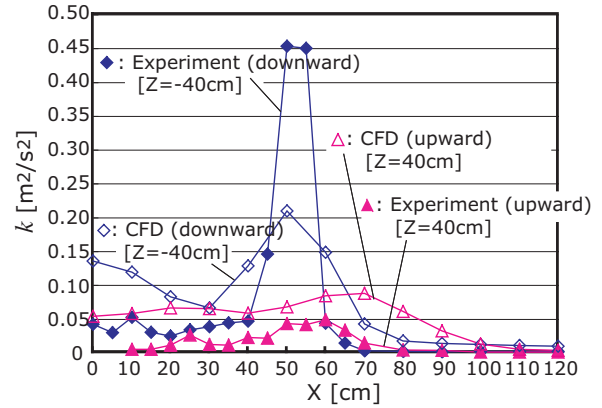


Fig.10 Turbulent kinetic energy distribution

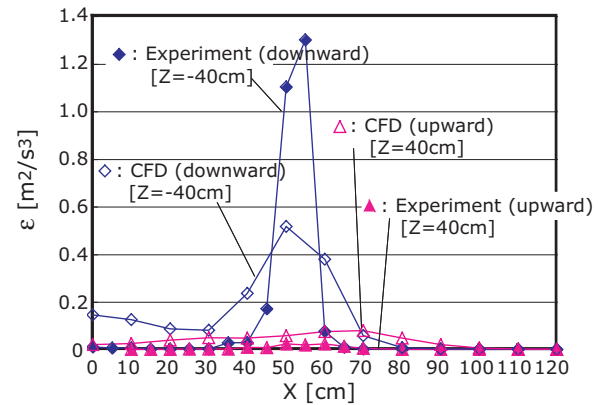


Fig.11 Dissipation rate of k distribution

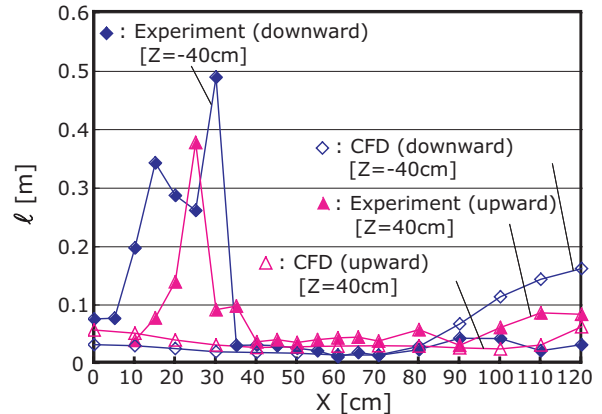


Fig.12 Turbulent length distribution

The CFD and measurement results of turbulent kinetic energy distribution and its dissipation rate distribution are shown in Fig.10 and 11, respectively. The CFD result was compared with the measurement result in blow-off side (at $Z=-40\text{cm}$ under downward airflow condition and at $Z=40\text{cm}$ under upward airflow condition). In the measurement result, they have tendency to become large significantly at $X=50\text{cm}$ to 55cm . On the other hand, although the maximum values in the CFD result have appeared in the almost same position as those in the measured result, they are smaller than the measured values. Since boundary conditions are equalized among the width of a mesh

(10cm), it is considered that non-uniform distribution like the measurement result is not observed in the CFD result. In the other positions, the values in the CFD result are larger than those in the measurement result. As a cause, the production of turbulent kinetic energy due to air velocity distribution may have been estimated too greatly.

Furthermore, since turbulent kinetic energy and its dissipation rate distribution of the CFD simulation differ from those of the measurement in this way, it is thought that the difference would induce air velocity distribution near the rotational center of the ceiling fan.

6.3 Turbulent length distribution

The CFD and measurement results of turbulent length distribution are shown in fig.12. Turbulent length is compared in blow-off side in the same way as turbulent kinetic energy and its dissipation rate. In the measurement result, it shows the maximum value at X= 25cm to 35cm. On the other hand, in the CFD result, its value is smaller than the measured value as a whole, and it becomes large in the distant position from the rotational center of the ceiling fan.

7. Conclusions

Air velocity near a ceiling fan was measured. Then the CFD simulations of the experimented space were performed using the boundary conditions of the ceiling fan based on air velocity measurement, and validity of the boundary conditions was examined by comparing the measurement result with the CFD result. The conclusions can be drawn as follows:

- The floor affects the airflow pattern greatly in the distant position from the ceiling fan.
- The measurement value and the CFD value were in good agreement about the suction airflow.
- Under the downward condition, air velocity near the rotational center of the ceiling fan in the CFD result was larger than that in the measurement result. As a cause, it is possible that large distribution resulting from the rotational cycle of the ceiling fan is also included in turbulent parameters given as boundary conditions and that the division interval of space is not fully fine.

In order to account for the influence of the division interval of space, CFD simulations with fine division are required. It may not be appropriate to input the value computed from the measurement result into CFD simulation as it is, and then the further examination is required about turbulent parameters given to the boundary conditions of the ceiling fan. Moreover, the size and position of the boundary surface should be examined, too.

More research would be needed to investigate the effect of the size of the computational grid and the turbulence parameters on the accuracy of the simulation with this airflow model.

Acknowledgements

The authors would like to thank Machiko Kuise for her help in carrying out the measurements and CFD simulations. The provision of the ceiling fan from Matsushita Ecology System Co., Ltd. is gratefully acknowledged.

Nomenclature

k	=	turbulent kinetic energy [m ² /s ²]
$\overline{u'^2}$	=	mean-square fluctuating component of velocity [m ² /s ²]
ε	=	dissipation rate of turbulent kinetic energy [m ² /s ³]
C_d	=	constant (0.09)
ℓ	=	turbulent length [m]
Λ	=	integral length [m]
\overline{u}	=	mean velocity [m/s]

References

- [1] F. H. Rohles, S. A. Konz and B. W. Jones. Ceiling Fans as Extenders of the Summer Comfort Envelope. *ASHRAE Transactions*, Vol.89 (1983), Part 1A, pp.245-262
- [2] S. Chandra. Fans to Reduce Cooling Costs in the Southeast. *Florida Solar Energy Centre FSEC-EN-13-85*, Cape Canaveral, FL, 1985
- [3] R. Aynsley. Fan Size and Energy Efficiency. *International Journal of Ventilation*, Volume 1 Number1, 2002
- [4] P.V. Nielsen. Description of Supply Openings in Numerical Models for Room Air Distribution. *ASHRAE Transactions* (1992): symposia.
- [5] STREAM ver.5, Software Cradle co. Ltd. <http://www.cradle.co.jp/eindex.htm>